Journal of Materials Chemistry C

Accepted Manuscript

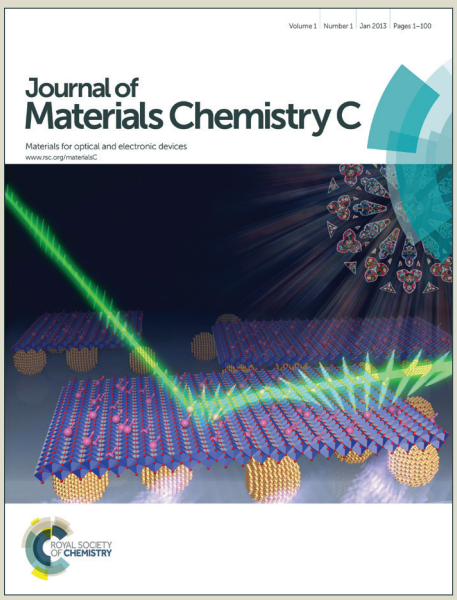

ROYAL SOCIETY OF CHEMISTRY

www.rsc.org/materialsC

Journal of Materials Chemistry C

ROYAL SOCIETY OF CHEMISTRY

ARTICLE

Recent progresses on the applications of graphene in surface-enhanced Raman scattering and plasmon-induced catalytic reactions

Received 00th January 20xx,
Accepted 00th January 20xx

DOI: 10.1039/x0xx00000x

www.rsc.org/

Jiayu Chu,†[a] Leilei Kang,†[a] Hongtao Zhao,[a] Ping Xu,*[a] and Mengtao Sun*[b]

Graphene continues to attract tremendous interest, owing to its excellent optical and electronic properties. On the basis of its unique features, graphene has been employed in the ever-expanding research fields. Surface-enhanced Raman scattering (SERS) may be one of the significant applied fields where graphene can make a difference. Since its discovery, SERS technique has been capable of ultra sensitively detecting chemical and biological molecules at very low concentration, even at single molecule level, but some problems, such as irreproducible SERS signals, should be overcome before practical application on spectra analysis. Graphene can be a promising candidate to make up the deficiency of conventional metal SERS substrate. Furthermore, graphene, serving as the enhancement material, is usually deemed as a chemically inert substance to isolate the interactions between metal and probe molecules. While, irradiated by laser, structure changes of graphene under specific conditions and the contributions of its high electron mobility in plasmon-induced catalytic reactions are often ignored. In this review, we mainly focus on the state-of-the-art applications of graphene in the fields of SERS and laser-induced catalytic reactions. The advances of informative Raman spectra of graphene are firstly reviewed. Then, the graphene related SERS substrates, including graphene-enhanced Raman scattering (GERS) and graphene-mediated SERS (G-SERS), are summarized. We finally highlight the catalytic reactions occurring on graphene itself and molecules adsorbed onto graphene upon laser irradiation.

1 Introduction

Graphene, a pioneer of two-dimensional (2D) materials, has attracted more and more attention since its discovery in 2004.[1] A perfect single layer of honeycomb matrix composed of sp^2 bonded carbon atoms endows it with many outstanding properties, such as high surface area, robust mechanical strength, superior thermal conductivity and electronic performance.[2] Graphene, on the basis of above-mentioned characteristics, has already been employed successfully in the ever-expanding research fields including, but not limited to, micro-nano electronic devices, energy storage, photoelectric detection, structural or functional reinforced composites.[3, 4]To date, many kinds of preparation methods have been developed to satisfy requirements of quality and quantity, including liquid phase and thermal exfoliation,[5, 6] chemical vapor deposition,[7] molecular beam epitaxy[8] and so forth. It is natural to consider exploring graphene for sensor applications by virtue of its extreme sensitivity to the surroundings. Thus, graphene-based devices have been exploited for fabricating sensors of strain, gas environment, pressure, magnetic field and optics.[9]

Surface-enhanced Raman scattering (SERS), as a significant optical technique of spectral analysis, is well-known for its ultra sensitivity, molecular fingerprint and rapid pre-treatment.[10] High-quality SERS spectra largely depend on the excellent SERS substrates with high enhancement factor, robust stability and acceptable reproducibility. In order to meet these requirements, a great deal of effort has been made in recent years. For traditional (plasmonic metal) SERS substrates, the mechanism of SERS can be classified into chemical and physical enhancement, where physical enhancement is induced by the strong interactions between light and metal nanostructures.[11, 12] However, these plasmonic metal SERS substrates possessing a supreme electromagnetic (physical) enhancement effect are vulnerable to limited stability and reproducibility, resulting in twinkling Raman signals.[13-15] Also, strong chemical interactions between SERS-active metal surface and probe molecules can partially induce fluctuant SERS responses.[16] Therefore, there is an obvious barrier to breakthrough before SERS can be widely used as a robust detection tool in practical applications. In such case, a new material is urgently expected to become the next promising SERS platform. Graphene, with apparently outstanding properties, could be an ideal alternative candidate for SERS substrates, as called graphene-enhanced Raman

a. Department of Chemistry, Harbin Institute of Technology, Harbin 150001, China. E-mail: pxu@hit.edu.cn; Fax: +86-451-8641-8750
b. Beijing National Laboratory for Condensed Matter Physics, Institute of Physics, Chinese Academy of Sciences, Beijing 100190, China. Email: mtsun@iphy.ac.cn.
†These authors contributed equally to this work.
DOI:10.1039/x0xx00000x

scattering (GERS).[17, 18] Due to the distinctive physical and chemical properties and ingenuity of structures, many advantages of graphene serving as SERS-active material have been highlighted by previous studies, depending on the unique electron and photon structures, atomic uniformity, biological compatibility, large delocalized π bond, and chemical inertness.[19]

Graphene, as a new member of SERS-active materials, would play a vital role in boosting the practical application of SERS technique in the near future. Notably, with the development of GERS, some catalytic reactions induced by the excitation source of SERS (i.e. laser) are also becoming of great interest since it may broaden applications of graphene and provide new insight into this kind of catalytic reactions. In this review, from many other unique properties of graphene, we only concentrate on its state-of-the-art applications in terms of SERS and plasmon-induced catalytic reactions.

2 Graphene-enhanced Raman spectroscopy

2.1 Raman spectroscopy of graphene

It is well-known that Raman spectroscopy is undoubtedly one of the powerful techniques for the characterization of graphene.[20, 21] Before discussing GERS phenomenon in detail, it is necessary to firstly understand the informative Raman spectroscopy of graphene itself. Fig. 1a (upper) shows the typical Raman spectrum of pristine graphene, in which there are two most intense Raman peaks at ~ 1580 (G band) and ~ 2700 cm^{-1} (G' band), resembling to that of graphite.[22] The G peak is responsible for the in-plane vibration of sp^2 hybridized C atoms, which is a sole first-order Raman scattering process in single layer graphene (SLG). In fact, G' band, as a second-order Raman scattering, has no direct connection with G band, which originates from absolutely different photonic interactions.[23] While such photons give rise to a peak at ~ 1350 cm^{-1} in defected graphene or the edge of perfect graphene, termed as D band, corresponding to the breathing modes of six-atom rings and requiring a defect to activate it (bottom of Fig. 1a).[24, 25] Since Raman shift of G' peak is usually twice that of D peak, G' peak is also known as 2D peak. Besides D band, D' band is another Raman characteristic relative to the defects of graphene, which is produced by double resonance through an intravalley process.[26]

After identifying Raman features of graphene, one can acquire abundantly helpful information ,such as the number of graphene layers[27], the types of defects and edges[28] as well as the doping level.[29] Apparently, SERS phenomenon is an obvious surface effect, that is, the number of graphene layers could immensely influence the enhancement factor, when using graphene as an SERS substrate. Therefore, we herein will emphatically discuss the determination of the number of graphene layers by Raman spectroscopy. Fig. 1b shows the optical image of graphene fabricated by mechanical exfoliation, and well-aligned edges of SLG, bilayer graphene (BLG), trilayer graphene (TLG) and four-layer graphene (4LG) can be distinguished clearly by their color contrasts. For better understanding, the corresponding schematic diagram is depicted in Fig. 1c.[30] Raman spectra show that the shapes and Raman shifts of G' band will change regularly with the number of graphene layers (Fig. 1d). It can be seen that G' band occurs a blue shift linearly with increase in the full width at half maximum (FWHM).[26] The G' band of SLG is a perfect single Lorentzian peak, while the G' peaks need to be fitted with different numbers of Lorentzian functions in multilayered graphenes. Furthermore, to ascertain the number of graphene layers, one has to refer to C mode at low frequency (~ 40 cm^{-1}) in the Raman spectra of multilayered graphene. Theoretically, the absence of C peak would be the most direct evidence of SLG since it is induced by relative motions of graphene planes and sensitive to the interaction of interlayers. In Fig. 1e, similar to the G' peak, the position of C peak also shifts to a higher wavenumber as a function of the number of graphene layers, which has been interpreted by the linear-chain model.[31] However, C peak is still not familiar to broad researchers because the low frequency of C peak could be beyond the notch and edge filter cut-off of many Raman spectrometers. In recent years, this problem has been solved by coupling a BragGrate filter with a single monochromator. Thus, C peak will be increasingly used as a direct evidence to investigate graphene or even other multilayered materials. Needless to say, these two (G' and C band) linear relations will be helpful to determine the number of graphene layers and accelerate the development of graphene-related SERS technique.

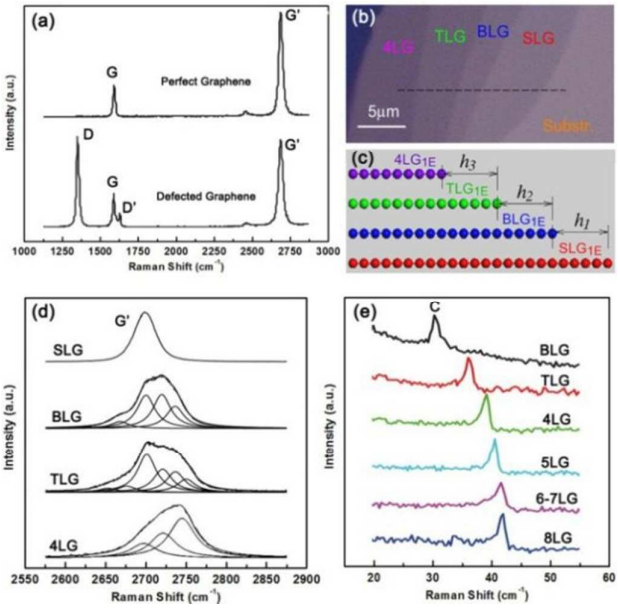

Fig. 1 (a) Raman spectra of perfect graphene (upper) and defected graphene (bottom); (b) Optical microscope image of graphene with different layers (from SLG to 4LG); (c) Schematic illustration of stack configuration at edge of graphene in (b); Evolution of G' band (d) and C band (e) with the number of graphene layers. Adapted from Nature Publishing Group and Elsevier.[25, 26, 30]

2.2 Graphene related SERS substrates

SERS technique enables ultrasensitive detection down to single molecule level, but is severely subjected to the interference of fluorescence, as the cross section of fluorescence (~10^{-16} cm^2) is

much larger than that of Raman scattering (~10^{-22}cm^2).[32] It was found that graphene was capable of quenching fluorescence of molecules[33] or even quantum dots,[34] which would be beneficial for collecting an ideal Raman spectrum without a waved fluorescence background. In this regard, photoinduced electron transfer mechanism and/or energy transfer mechanism have been developed.[35-37] Schematic diagram of using graphene as an efficient substrate for quenching the fluorescence of Rhodamine 6G (R6G) was shown in Fig 2a. With the excitation of 514 nm laser, only an intensely fluctuant fluorescence background was obtained in R6G solution at a concentration of 10 μM, where Raman peaks of R6G were covered absolutely. In contrast, a high-quality Raman fingerprint spectrum of R6G could be obtained on SLG, given the same excitation source (Fig. 2b). One note is that the emergence of Raman peaks of R6G is contributed to the immense quenching of fluorescence with the assistance of SLG. Furthermore, it was verified that fluorescence background could be suppressed about 3 orders of magnitude by employing graphene as a fluorescence quencher, leading to obvious Raman signals due to the improvement of signal-to-noise ratio.[38] From then on, graphene began to come into the SERS field and became an indispensable figure.

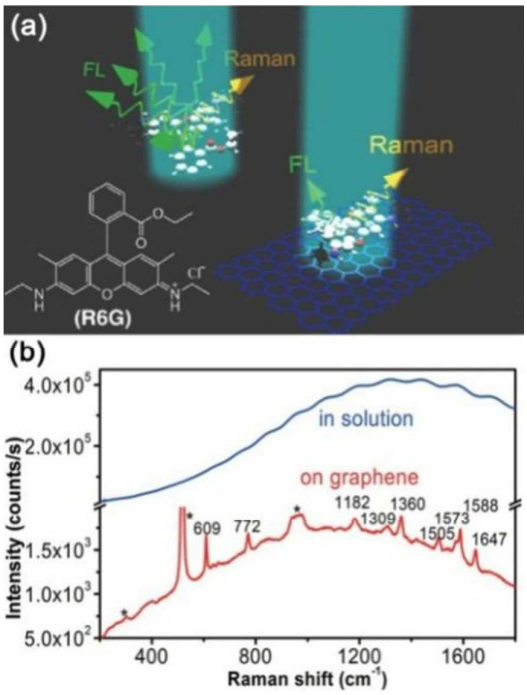

Fig. 2 (a) Schematic illustration of graphene to quench fluorescence of organic dye R6G; (b) Comparison of Raman spectra of R6G dissolved into water (upper) and absorbed onto SLG (bottom). Adapted from American Chemistry Society.[38]

2.2.1 Graphene/metal hybrid structures as SERS substrates

As known, SERS phenomenon was initially found on the roughened Ag electrode, where the Raman signal of pyridine was immensely magnified due to the presence of intense electromagnetic field.[39] Therefore, preparing tailored plasmonic-metal nanostructures has been the main subject of SERS study in the past few decades.[40-45] However, it is still a great challenge for SERS technique to meet the requirements of practical applications, since the developed metal substrates still suffer from poor stability and reproducibility.[46] Most SERS signals usually originate from a few so-called "hot spots" (eg. nanotips, nanogaps) unevenly distributed over the surface of metal SERS substrates.[47] Graphene, with unique properties coupled with plasmonic metal nanostructures, would furnish an intriguing hybrid system with various electro-optic properties, which might promote the development of SERS substrates. Moreover, It is also worthy to note that

I. Graphene as a probe of SERS

Actually, the role of graphene in SERS is versatile, which can be used as not only enhancement material but also target analyte.[48, 49] Before discussing graphene/metal hybrids, we will firstly introduce some typical studies concerning the interactions between graphene and plasmonic metal by Raman spectroscopy, namely graphene as a probe. With obvious specific Raman bands and fluorescence quenching, graphene can be competent enough as a SERS reporter.

Shin's group collected the Raman signals of SLG, BLG and TLG by depositing Ag nanoparticles onto the graphene surface.[50] It was found that the D band of graphene was split into two bands, the extent of which was decreased with increasing the number of graphene layers. Therefore, besides 2D and C band, the splitting of D band in SERS can also be employed to determine the number of graphene layers. In particular, the SERS enhancement factor also followed the variation tendency of D band. Furthermore, the electronic states of doped graphene were determined according to the peak shift of G and 2D bands due to the metal deposition onto graphene. Nevertheless, the SERS enhancement factor is rather low (~ 24 for SLG) in this system. To improve the enhancement factor, Wang et al fabricated an Au film with hexagonally ordered Au nanopyramids by nanocasting, and subsequently an SLG was covered over them, as shown in Fig. 3a. [51] The lateral and top view of SEM images gave a clear morphology of SLG coated Au tips (Fig. 3b and c). The dashed circle in Fig. 3c highlighted the folded graphene between Au tips, which was deemed as the origin of a new set of D band (D' band) in the Raman spectrum. In fact, D' band comes from a double resonance process (as discussed in Section 2.1). Raman spectra measured from three different substrates were compared in Fig. 3d, in which the Raman signal from Au tips was strongest among them, indicating the existence of strong interactions between SLG and Au tips. In addition, the enhancement factor of Au tips was calculated to determine its SERS performance, and the enhancement factor of this novel graphene/Au system could be up to 10^7. Also, the distribution of SERS "hot spots" over Au nano arrays could be visible by superimposing the Raman mapping and SEM image in the same region (Fig. 3 e and f). With this high Raman enhancement factor, the plasmonic metal / graphene hybrids could be explored as a new type of SERS substrates for sensitive molecule detection, termed as graphene-mediated SERS (G-SERS) technique. Subsequently, it was demonstrated that this G-SERS substrate was capable of realizing an ultrasensitive detection at single molecule level and providing uniform SERS response in their follow-up work.[52]

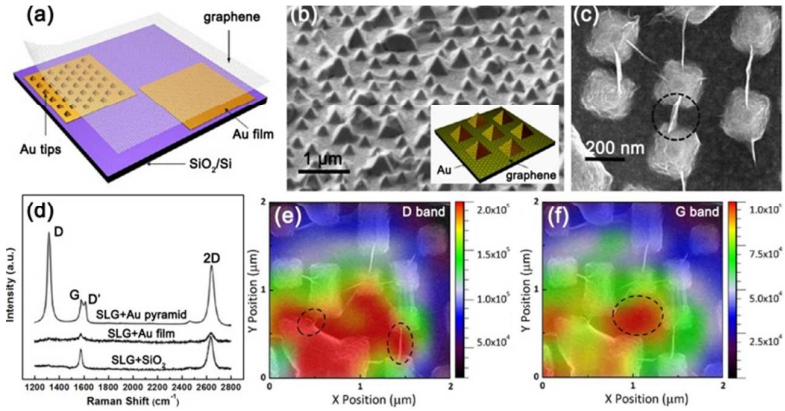

Fig. 3 (a) Schematic illustration of the constructions of SLG/Au pyramid, SLG/Au film and SLG/SiO_2; (b) SEM image of Au pyramid covered with SLG; (c) Top view of hexagonally arranged arrays of Au tips with sharply folded graphene in SEM; (d) comparisons of Raman spectra of SLG from different substrates (Au tips, Au film, and SiO_2); The superposition images of Raman mapping depending on the intensity of (e) D band and (f) G band and SEM image in the same region. Raman spectra and mappings are excited by 633 nm laser. Adapted from American Chemistry Society.[51]

II. Graphene-mediated SERS substrates

The intense interactions between graphene layer and plasmonic metal structures are expected to combine the virtues of themselves for SERS detection. For example, Losurdo's work reported that graphene could be an electron shuttle for silver deoxidation, ensuring the high SERS performance of Ag nanostructures over a long time period.[53] Zhang's group developed a graphene/metal hybrid SERS substrate with comparable SERS enhancement factor,[54] which consisted of SLG and tape supported Au/Ag nanoislands. Nanogaps among metal nanoislands and SLG provided a huge electromagnetic enhancement and an atomically uniform SERS-active surface. As-prepared graphene/mental hybrid material was employed as an efficient G-SERS substrate to detect R6G and CuPc. Signals from G-SERS substrate were stable and reproducible, compared to normal plasmonic metal SERS substrates. In a similar complex, they found that the enhancement factor could be immensely increased after thermal treatment.[55] Schematic illustration of graphene-veiled gold film with nanoislands before annealing was shown in Fig. 4a, where graphene laid on the surface of nanoislands. After annealing, Au nanoislands tended to aggregate into larger nanoparticles, while flat graphene layer became wrinkled, resulting in the change of contact state of former nanoislands (Fig. 4d). In this process, the "hot spots" could be produced and electromagnetic enhancement could also be enormously improved, as illustrated in Fig. 4b and e. This hypothesis could be confirmed by a tremendous enhancement in the G-SERS of CuPc from BLG-veiled Au aggregations, comparing to that of BLG-covered nanoislands before annealing (Fig. 4c and f). Furthermore, it was verified that the annealed G-SERS substrate with comparable enhancement factor was more stable than plasmonic metal SERS substrates.

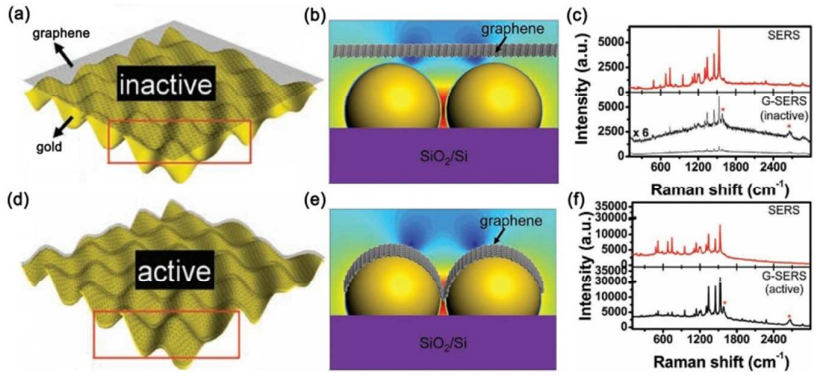

Fig. 4 Schematics of graphene-veiled gold film with nanoislands (a) before and after (d) annealing at 400 ^{o}C for 2 h; (b, e) The distribution of electromagnetic field between a gap of graphene-coated nanoislands that correspond to the red rectangle marked region in (a, b), respectively; SERS and G-SERS spectra of R6G collected from (c) before and (f) after annealed nanoislands and BLG-veiled islands. Adapted from American Chemistry Society.[55]

Different with previous studies, Zhu et al. transferred SLG onto a large-area Au nanovoid arrays (GNVAs) to investigate the enhanced light-matter interactions.[56] Fig. 5a showed the SEM image of graphene covered GNVAs, where the dark region was coated with graphene. To further understand the contact form between graphene and Au nanovoids, the insets gave an SEM image and schematic illustration of the cross-section of graphene covered GNVAs, where one could see that the graphene layer was suspended over the Au nanovoids. The enhanced light-matter interactions could be evidenced by the evolution of the measured reflection spectra of GNVAs and graphene covered GNVAs. As shown in Fig. 5b, the plasmonic resonance of GNVAs became shallower, broader, and red-shifted after covering graphene, which could be ascribed to the presence of graphene and the graphene

Ohmic loss. Further analysis showed that the optical absorption of GNVAs could be increased by as high as 30% by covering SLG. The Raman intensity of SLG on GNVAs was much stronger than that on Si/SiO_2, further indicating the existence of strong interactions between SLG and GNVAs (Fig. 5c). Of course, the hybrid nanostructure composed of flat graphene and GNVAs was naturally considered to be an ideal SERS substrate. As shown in Fig. 5d, Raman spectra of R6G collected from SLG-covered GNVAs were well consistent with that of bulk R6G. However, many newly formed and irreproducible bands appeared in the Raman spectra of R6G adsorbed on GNVAs without SLG (highlighted by red arrows in Fig. 5d). These changes may originate from a photochemical process, because gold is a good catalyst in traditional catalytic filed. That means the presence of graphene can protect R6G molecules from laser-induced decomposition, getting rid of the chemical activity of plasmonic metal surface. However, graphene is not always a universal guardian for all chemical species. We will discuss the related studies in terms of graphene-containing laser-induced chemical reactions in the next part.

Recently, more complicated metal-graphene systems have been developed to obtain more reliable and sensitive SERS readout, namely multi-dimensional plasmonic coupling structures, where graphene is commonly used as a dielectric gap to adjust the localized plasmonic resonance between metal layers.[57-60] Zhao et al. designed and fabricated an Au nanoparticle–graphene–Ag nanoparticle complex as highly sensitive SERS substrate by exploiting its multi-dimensional plasmonic coupling. [61] Fig. 6a shows the simulation configuration of Au-SLG-Ag hybrid structure on a quartz wafer. It can be seen that SLG is sandwiched between two kinds of metal nanoparticles. And the strong electric field mainly resides in the gaps separated by SLG (Fig. 6b). To detect Rhodamine B (RhB) of 10^{-7} M, the strongest Raman signal is collected from Au-SLG-Ag complex, indicating the superiority of this well-designed multi-dimensional plasmonic coupling structure (Fig. 6c). Fig. 6d shows that the detection limit of the Au nanoparticle–graphene–Ag nanoparticle complex can reach as low as 10^{-11} M.

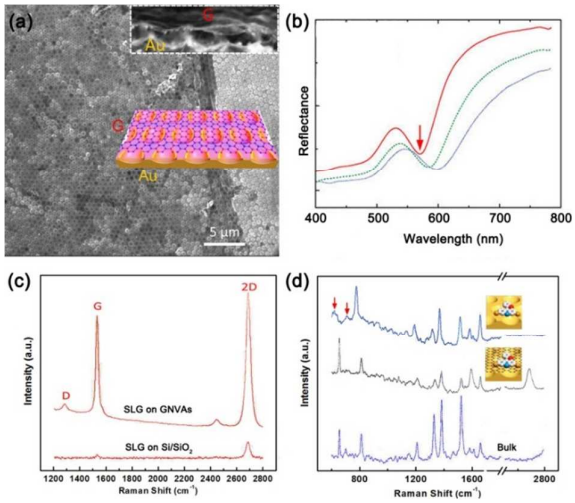

Fig. 5 (a) SEM image of a large-area nanovoid arrays covered with SLG. The insets show a SEM picture and schematic of the cross-section of graphene covered nanovoids; (b) Reflection spectra of nanovoid arrays before (the solid red lines) and after deposition of monolayer (the dashed green lines) and bilayer graphene (the dotted blue lines); (c) Raman spectra of a SLG on different substrates; (d) Comparison of Raman spectra of bulk R6G and R6G adsorbed on SLG veiled and bare GNVAs. Adapted from American Chemistry Society.[56]

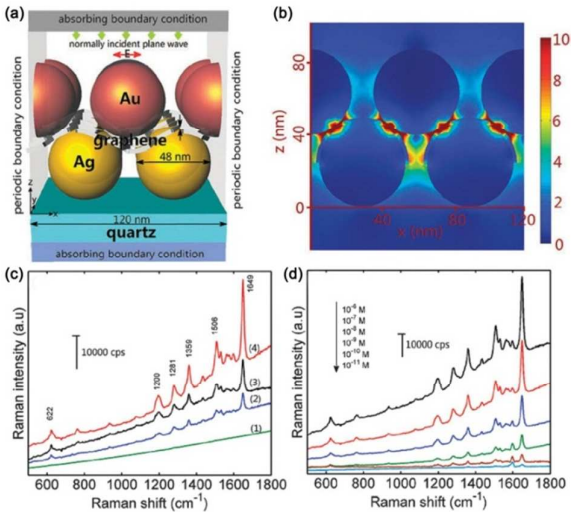

Fig. 6 (a) simulation configuration of Au-SLG-Ag on a quartz wafer; (b) the intensity distribution of electric field simulated by finite element method; (c) Raman spectra of RhB at a concentration of 10^{-7} M on quartz (1), 8 nm Ag (2), 8 nm Au/8 nm Ag (3) and 8 nm Au/1LG/8 nm Ag (4), respectively; (d) concentration-dependent SERS spectra collected from the 8 nm Au/1LG/8 nm Ag complex. Adapted from Royal Society of Chemistry.[61]

In this part, some typical works involving graphene/metal hybrid nanostructures as SERS substrates were reviewed. Besides gold nanostructures, silver and copper nanostructures coupled with graphene have also been reported.[59, 62-64] As an ever-growing research field, a large number of researchers have been focusing on engineering and developing new G-SERS substrates to overcome drawbacks in plasmonic metal SERS substrates.[64-68] Developing graphene/metal hybrid nanostructures as SERS substrates would be a promising way to reveal potential enhancement mechanism and meet application requirements.

2.2.2 Pure graphene as SERS substrates

Exploiting pure graphene as SERS substrate is also called graphene-enhanced Raman scattering (GERS). GERS has many distinct advantages, including high chemical stability, homogeneous surface and exclusive chemical enhancement, even though its enhancement factor is usually ranged from less than 10 to 10^3.[69] Many drawbacks of conventional SERS method could be overcome through developing GERS technique. For instance, quantitative detection is almost impossible on plasmonic metal related SERS substrates, because the location and orientation of molecules are difficult to be well controlled. However, graphene with highly homogeneous surface would provide a uniform environment for adsorbed molecules, making quantitative analysis accessible.

In 2010, Ling et al firstly discovered and studied the feasibility of utilizing the mechanically exfoliated graphene as a SERS substrate.[17] The schematic illustration of Raman scattering from the molecules adsorbed on SLG was shown in Fig. 7a. Resembling the previous study concerning about graphene as a superior fluorescence quencher, an intense background submerged the Raman spectrum completely when R6G molecules were adsorbed onto SiO_2/Si substrate (Fig. 7b). On the contrary, Raman characteristics of R6G was perfectly presented on SLG, given the same experimental conditions. To determine the detection limit of the as-prepared

graphene substrate, concentration-dependent Raman studies were carried out (Fig. 7c). It was shown that on the monolayer graphene, one can detect R6G molecules with a concentration as low as 10^{-8} M, which is almost comparable with the detection limit of some plasmonic metal SERS substrates. Moreover, the influence of the number of graphene layers on Raman enhancement were also investigated, showing that Raman signals of all target molecules (phthalocyanine, R6G, protoporphyin IX and crystal violet) were decreased with an increase in the number of graphene layers.[70]

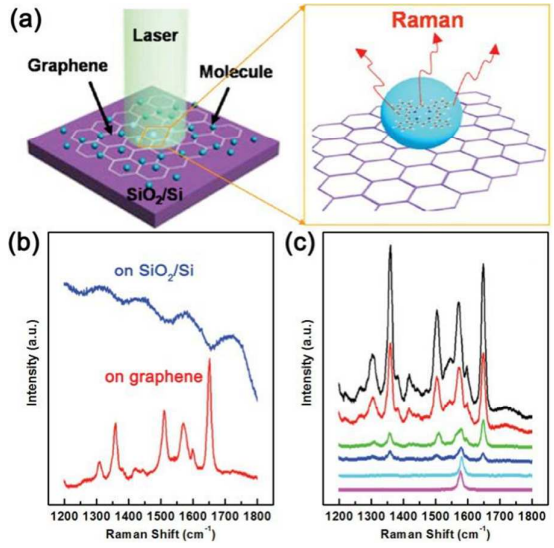

Fig. 7 (a) Schematic illustration of Raman scattering from the molecules adsorbed onto SLG; (b) comparison of Raman spectra of R6G on graphene and SiO_2/Si substrate; (c) Concentration-dependent Raman spectra of R6G using SLG as a substrate. The concentrations from top to bottom are 4×10^{-5},8×10^{-7},8×10^{-8},8×10^{-9},8×10^{-10}, and 8×10^{-11} M, respectively. Peaks labelled with asterisk are G band of graphene. Adapted from American Chemistry Society.[17]

In the last, paragraph, we reviewed typical SERS phenomenon from pristine graphene. It is quite natural to consider using defected graphene as SERS substrate. Huh et al. fabricated a large-scale graphene by chemical vapor deposition (CVD), and then introduced defects (oxygen-containing functional groups) by UV/ozone-based oxidation methods to serve as efficient SERS platform.[71] Fig. 8a showed the photograph of CVD-grown large-scale graphene on glass and schematic illustration of detecting R6G utilizing pristine and oxidized graphene as SERS substrates, respectively. Inset indicated that the p-doped graphene was prepared after UV/ozone treatment, resulting in the down-shifting of the Fermi energy. It was suggested that the tunable SERS effect could be achieved by modulating electron transport property of graphene. Fig. 8b displayed the evolution of Raman spectra of graphene with the UV/ozone exposure time. After 5 min, a large amount of defects had been introduced into the graphene, as evidenced by the appearance of the strong D band. The intensity of Raman spectrum of R6G on oxidized graphene was obviously stronger than that on untreated graphene (Fig. 8c). The enhancement factor of the oxidized graphene SERS substrate was calculated to be ~10^4, which was one order of magnitude larger than that of pristine graphene. In this regard, two possible reasons were proposed to explain this: (1) the oxygen functional groups on graphene surface and (2) the p-type doping of the graphene. On one hand, the production of oxygen-containing groups on graphene surface have larger polarizability and stronger dipole moment, which is beneficial to enhancing localized electric field. On the other hand, compared to the pristine graphene, the p-doped graphene possessing lower Fermi level would improve Raman signals of dye molecules adsorbed onto the graphene surface. In addition, GERS effects on graphite oxide (GO),[72] meshed graphene,[73] graphene edges[74] have also been investigated systematically. It is clear that these studies have laid a solid foundation for us to further understand the enhancement mechanisms of GERS.

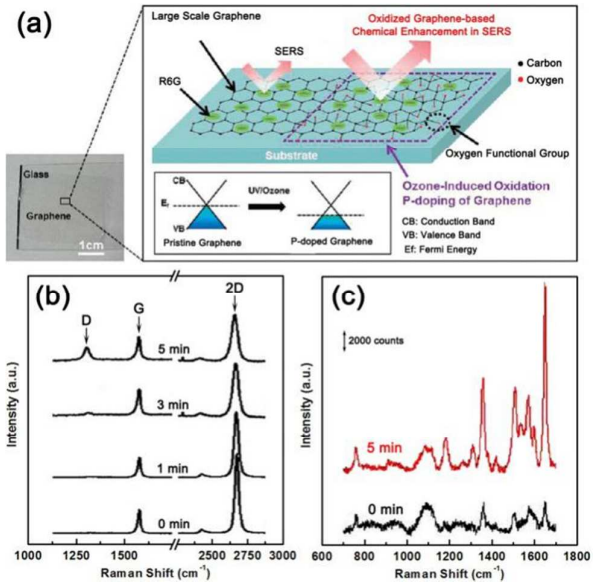

Fig. 8 (a) Photograph of CVD-grown large-scale graphene on a glass and schematic illustration of detection of R6G using pristine and oxidized graphene as SERS substrates, respectively (Inset shows the down-shifting of the Fermi energy of the graphene after UV/ozone treatment); (b) Changes of Raman spectra of graphene as a function of the UV/ozone-induced oxidation time periods; (c) Raman spectra of R6G from the graphene before and after 5 min ozone treatment. Adapted from American Chemistry Society.[71]

Previous studies have reported that the enhancement factor of GERS is very distinct for different probe molecules.[75] Recently, Huang et al. confirmed this molecule effect, namely molecular selectivity of GERS.[76] This amplitude of variation could be as large as 2 orders of magnitude for various molecules. Fig. 9a showed the schematic illustration of the molecular selectivity of GERS for different types of molecules. Two sets of molecules were elaborately selected to investigate the influence of the molecular energy levels and structures on GERS. The molecules in the first group had similar molecular structures but different energy level, including copper phthalocyanine (CuPc), zinc phthalocyanine (ZnPc), and Copper(II)1,2,3,4,8,9,10,11,15,16,17,18,22,23,24,25-exadecafluoro-29H,31H-phthalocyanine (F16CuPc) (Fig. 9b). The another group contained molecules with similar energy levels but different molecular structures, involving tetrathienophenazine (TTP), tris(4-carbazoyl-9-ylphenyl) amine (TCTA), and 2, 2', 7, 7' -tetra(N-phenyl-1-naphthyl-amine)-9,9'-spirobifluorene (sp2-NPB) (as shown in Fig. 9c). By comparing the Raman enhancement factors of these two classified molecules, it was found that: (1) an intense Raman enhancement would occur if Fermi level of graphene filled exactly

in between the highest occupied molecular orbital (HOMO) and lowest unoccupied molecular orbital (LUMO) energy of a molecule; (2) strong GERS enhancement preferred to produce from these molecules with molecular symmetry and substituent similar to that of graphene structure. Moreover, many other factors affecting the GERS effects have also been reported, such as the influence of graphene Fermi level,[77] first-layer effect,[78] external electrical field,[79] molecular orientation,[80] interface interactions[18] and doping states.[81]

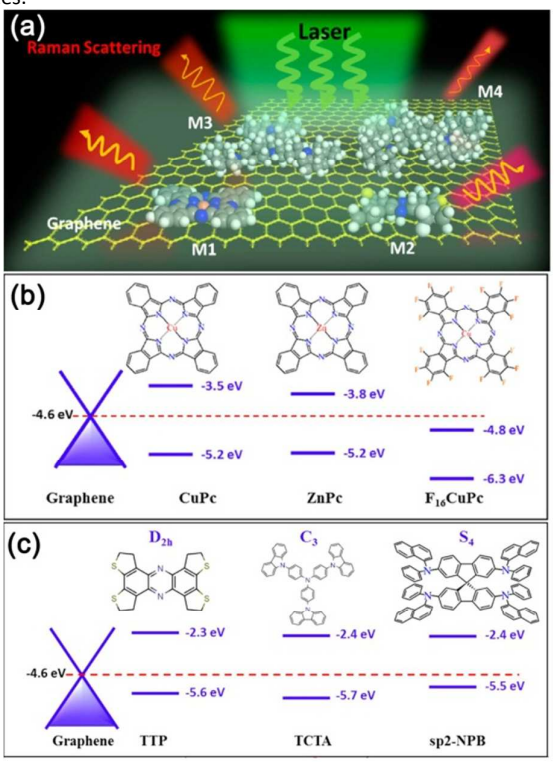

Fig. 9 (a) Schematic of the molecular selectivity of GERS for different kinds of probe molecules (M_1, M_2, M_3, M_4); Molecular structures of (b) CuPc, ZnPc and F16CuPc, (c) TCTA, TTP, and sp2-NPB, as well as the relative energy levels of the Dirac cone of graphene and the corresponding molecular HOMO/LUMO. Adapted from American Chemistry Society.[76]

Driven by the rapid development of graphene, other 2D materials such as molybdenum disulfide (MoS_2), boron nitride (BN), likewise become increasingly intriguing because of their specific properties.[82, 83] Ling et al found that MoS_2 and hexagonal boron nitride (h-BN) also had Raman enhancement effect, other than graphene. The Raman enhancement effects were compared by using the copper phthalocyanine (CuPc) molecule as the analyte.[84] Schematic illustration of fabrication and Raman measurement method was depicted in Fig. 10a. Given the same measurement conditions, Raman spectra of CuPc from different substrates were shown in Fig. 10b. The Raman characteristics of CuPc on graphene, MoS_2 and h-BN were clearly observable, while Raman signal from blank SiO_2/Si was almost negligible. Further analyses demonstrated that the enhancement factors varied on graphene and h-BN, depending strongly on the vibrational modes of CuPc. The weakest Raman enhancement was collected on MoS_2 among these three 2D materials. It was believed that these diversities were caused by the different electronic and chemical properties of these substrates. Graphene, with nonpolar C−C bond, is a zero-gap semiconductor, which facilitates charge transfer between probe molecules and graphene surface. For h-BN, strong dipole−dipole coupling may occur since h-BN involves a strong B−N bond, but it is an insulator. MoS_2, as a semiconductor with a polar covalent bond (Mo−S), would lead to both charge transfer and dipole−dipole coupling, yet its collective enhancement effect is weaker in magnitude. This work demonstrated that, besides graphene, other 2D materials could also be explored as the potential substrate in SERS.

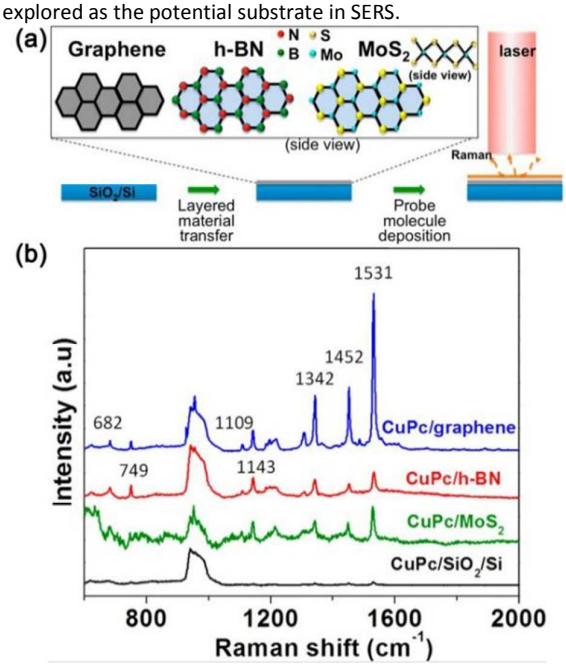

Fig. 10 (a) Schematic diagram of fabrication and measurement method of 2D Raman enhancers; (b) Comparison of Raman spectra of CuPc molecule collecting from different substrates. Adapted from American Chemistry Society.[84]

To date, charge transfer (chemical enhancement) and electromagnetic enhancement (physical enhancement) have been widely accepted as two main SERS enhancement mechanisms, where the latter one is predominant.[85, 86] Electromagnetic enhancement has been widely explained by theoretical models and experimental results. As for chemical enhancement mechanism, the coexistence of both physical and chemical enhancement is difficult to ascribe their contributions while using traditional plasmonic metal SERS substrates, since the effect of charge transfer is always engulfed by the overwhelming electromagnetic enhancement.[87] An atomic flat surface is necessary if one wants to study the chemical enhancement, but it is usually difficult to realize under general experimental conditions. For graphene, its surface plasmon is in the range of hertz, which easily rules out the effect of electromagnetic enhancement in visible range.[88] Thus, the utility of graphene as SERS substrates has opened up a bright way to approach deep insight into chemical enhancement. However, the existence of GERS effect had been controversial in GERS research history. For example, Thrall et al declared that the sensitive Raman detection of graphene was mainly due to the strong quenching of fluorescence, but no obvious Raman enhancement was found in their study.[89] Nevertheless,

GERS phenomenon originates from chemical enhancement, which has reached a consensus up to now.

The earliest and the most widely used theory to interpret chemical enhancement is vibronic coupling theory, which is proposed by Lombardi et al. based on Albrecht's theory.[90] This theory is only suitable for systems with intense interactions between molecules and surfaces. In 2006, Persson et al. developed an alternative theory for nonresonant SERS effects by elucidating the change of the surface polarizability.[91] To better understand the chemical enhancement of GERS, Barros et al proposed a general theoretical model recently, namely third-order time-dependent perturbation theory, to describe the chemical enhancement on 2D surfaces, especially for graphene.[92] In this work, the graphene Fermi level, molecular HOMO/LUMO, phonon and laser energies are considered to be relative to the enhancement factor of GERS. It has been suggested that for ideal 2D metal surface, SERS effect will occur when the Fermi level of metal surface is close to the HOMO or LUMO of the molecules. Once Fermi energy of surface exactly matches with either the HOMO plus or LUMO minus the energy of the excitation source, the strongest SERS signals will be collected. Graphene is deemed as a special 2D material that enhanced Raman signal can be obtained when its Fermi level locates in the range of HOMO and LUMO of the molecules, which is consistent with some of the experimental results in ref. 76.

3 Laser-induced reactions on graphene

Graphene is expected to be an ideal building block for SERS substrates because of its unique properties. Beyond atomically uniform surface, graphene is capable of furnishing a chemically inert protective layer to prevent probe molecules from photoinduced catalytic reactions in the presence of plasmonic metal.[19, 56] Graphene is used as a mediator to cut off the chemical interactions between analytes and metal surfaces. However, laser serving as the excitation source of Raman spectrometer usually bring about some unexpected impacts owing to its strong light intensity. For example, SERS technique was initially regarded as a noninvasive detective method since it was discovered,[93] but it was found that the so called "evidences of chemical enhancement" was attributed by the newly produced chemical species.[94, 95] Since then, a great number of theoretical and experimental studies of surface plasmon mediated chemical reactions were reported.[96-102] Similarly, as research continues, it was found that graphene is not always an inert substance. The exotic atoms or groups modified graphene can be obtained by laser or photo irradiation, which will somewhat influence the SERS responses of probe molecules adsorbed onto it.[71] And some of plasmon-driven catalytic reactions occurring on the metal surface can also be triggered on graphene-coated metal SERS substrates.

3.1 Laser-induced surface modifications of graphene

So far, various approaches have been employed to alter the structures of graphene to further explore its novel properties. Chemical modification is one of the most common methods, including hydrogenation,[103] fluorination,[104] chlorination,[105, 106] methylation,[107, 108] phenylation.[109] Compared with other chemical methods, light-induced modification is a relative mild approach to functionalize and modulate band structure of graphene. The conducting π-bands and energy gap are varied obviously in this process, since the addition of exotic atoms or groups to the conjugated structure of graphene can lead to structural transformation of the C-C bonds from sp^2 to sp^3 hybridization.

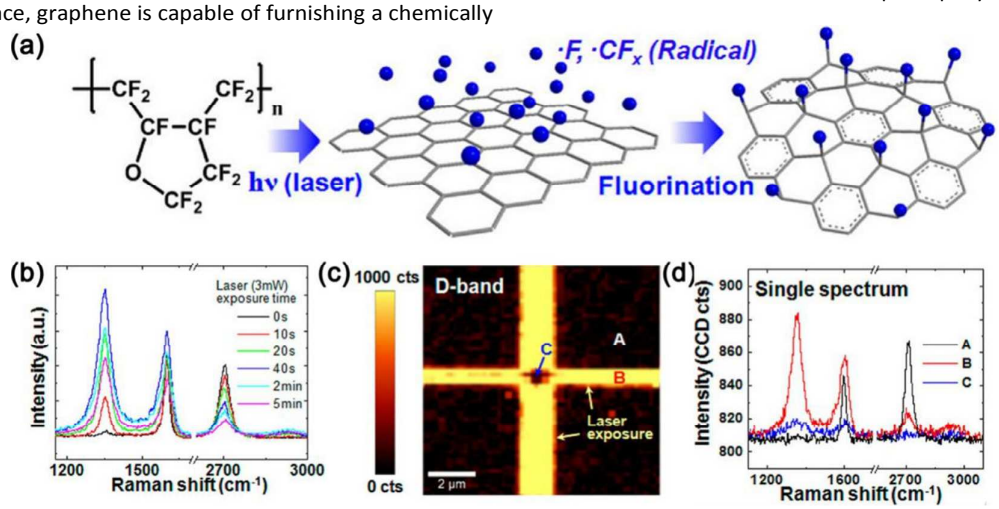

Fig. 11 (a) Schematic illustration of the mechanism of fluorination of graphene in the presence of CYTOP and laser illumination; (b) Evolution of Raman spectra of graphene as a function of laser irradiation time; (c) Raman mapping depending on D band (1300-1500 cm^{-1}).The spots marked with A, B and C represent three different regions in the CYTOP mask; (d) Raman spectra of graphene from three independent spots marked in (c). Adapted from American Chemistry Society.[104]

Ruoff et al reported that controlled fluorination of graphene could be achieved by utilizing the solid fluorin (CYTOP) and laser irradiation.[104] Fig. 11a illustrates the mechanism of fluorination of graphene, where fluorin-containing radicals play a vital role. The fluorination reaction of graphene was monitored by Raman spectroscopy along with the laser irradiation (Fig. 11b). It was found that the intensity of the characteristic D band at 1350 cm^{-1} was increased as the laser radiation increased within 40 s. Inversely, the intensity of 2D band around 2700 cm^{-1} was decreased gradually. These changes indicated that the perfect sp^2 bonded network in graphene had been damaged by laser irradiation. Because the fluorination of graphene was sensitive to laser illumination, the

regions of fluorination in graphene surface could be patterned. Raman mapping of the D band was carried out to observe the fluorination pattern (Fig. 11c). Three spots from different regions in Fig. 10c were selected to study the differences in Raman spectra (Fig. 11d), where A, B and C meant different regions of graphene covered with CYTOP mask. The independent spectra were well consistent with the time-dependent Raman spectra in Fig. 11b, indicating the most disordered structures was introduced at the center of cross pattern (spot C) upon an overlapping illumination.

Notably, the resistance of graphene was dramatically decreased after fluorination, which could be exploited as graphene devices. Likewise, the chlorination of graphene can be realized by UV light. Liu's group reported that chlorine radicals produced by xenon lamp radiation in the presence of Cl_2 could covalently attach onto the basal carbon atoms of graphene.[105] The chlorinated graphene exhibited similar electronic property with fluorinated graphene, and the resistance of chlorinated graphene could be increased by 4 orders of magnitude.

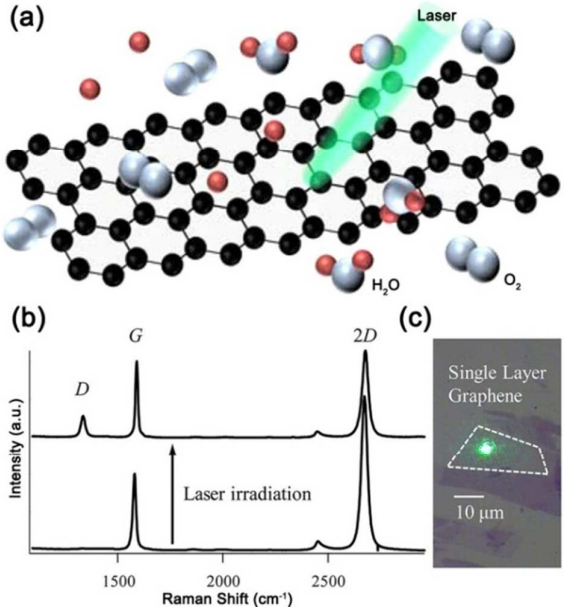

Fig. 12 (a) Schematic illustration of laser-induced oxidization of graphene in the surrounding environment of O_2 and H_2O vapor; (b) Comparison of Raman spectra of graphene before and after laser irradiation for 5 h; (c) Optical microscope image of SLG upon green laser irradiation. Adapted from American Chemistry Society.[110]

O_2 and H_2O vapor are necessary components in air, which are considerably active chemical molecules. Since most SERS experiments are conducted in an open system, the involvement of O_2 and H_2O molecules should not be ignored.[13, 111] For graphene mediated SERS substrates, chemically inert graphene exposed in air could also be vulnerable upon laser irradiation, resulting in unexpected changes in SERS spectra. Tanigaki et al discovered that laser irradiation could trigger a photochemical reaction on graphene in an ambient condition (Fig. 12a).[110] Fig. 12b showed Raman spectra of SLG before and after laser irradiation for 5 h. The emergence of D band as well as Raman shifts of G band and 2D band in the Raman spectrum of laser illuminated SLG confirm the successful introduction of oxygen-containing groups. To minimize the influence of graphene edges, test point was selected on the basal of large-area SLG (Fig. 12c). What's more, this effect is more obvious with the assistance of metal, which would be influential in Raman signals from G-SERS substrates. It should be mentioned that laser-induced reduction of graphene oxides has become an important method to prepare graphene-based materials in large scale.[112, 113] For this reversible photochemical process, researchers should carefully control the experimental conditions to acquire the desirable results.

3.2 Plasmon-driven catalytic reactions on graphene

Serving as a promising SERS enhancer, most of the previous studies were usually concentrated on its chemically inert surface free from metal-molecule interactions. However, the function of high electron mobility of graphene on charge transfer was often ignored during SERS measurement. In particular, the complex interactions among molecule, graphene, and metal processes have not been well understood.

Sun et al. carefully designed an Ag bowtie nanoantenna arrays (ABNA) substrate covered with controlled graphene layers to study a typical plasmon-driven catalytic reaction, transforming para-aminothiophenol (PATP) to p,p'-dimercaptoazobenzene (DMAB), aiming to reveal the charge transfer mechanism between PATP and graphene-covered Ag nanostructures.[114] Schematic illustration of plasmon-driven catalytic reaction of transforming PATP to DMAB on SLG-coated ABNA was depicted in Fig. 13a. SEM image of graphene-covered ABNA showed that uniformly ordered ABNA was veiled with large area graphene, which could protect Ag nanostructures from surface corrosion (Fig. 13b). It had been manifested that PATP molecules were vertically adsorbed onto the surface of plasmonic metal by thiol group, while anchored onto graphene in a paralleled manner due to the delocalized π bond (Fig. 13 c and d). It was suggested that the introduction of SLG would induce a strong dipole accelerating the charge transfer between PATP and graphene. This was supported by the in situ Raman spectra of PATP upon laser illumination, in which the ratio of I_{nn}/I_{cc} was used to evaluate the reaction progress (Fig. 13 e and f). Here I_{nn} means the Raman intensity of N=N bond of DMAB at 1440 cm^{-1} and I_{cc} is intensity of C-C bond at 1590 cm^{-1}. To attain the same value of I_{nn}/I_{cc} (1.21), the reaction time could be shortened to 1 min on SGL-covered ABNA, comparing to 11 min on pure ABNA. However, BLG-covered ABNA brought a negative effect. In this regard, the charge densities of PATP on bilayer graphene on Ag cluster were calculated. Electrons could only efficiently transfer to the top of the bilayer graphene, but not to Ag cluster and the bottom of the bilayer graphene. Therefore, this plasmon-driven catalytic reaction was suppressed on BLG-covered ABNA. Nevertheless, this demonstrated that graphene could be explored as a accelerator in plasmon-assistant catalytic reactions rather than just an inert protector. Moreover, graphene/Au hydrogel was prepared to serve as an efficient catalyst, exhibiting excellent catalytic performance towards the reduction of para-nitrophenol (PNP) to para-aminophenol (PAP). This high performance could be rationalized by the synergetic effect of graphene, that is, the high adsorption ability of graphene towards PNP and fast electron transfer from graphene to Au nanoparticles. This may be helpful to interpret the phenomenon relevant to graphene-assisted plasmon-driven catalytic reactions. Recently, Liang et al synthesized graphene/Au nanocomposites through in

situ chemical reduction method as a SERS substrate to monitor the plasmon-driven surface-catalyzed reaction from para-nitrobenzenethiol (PNBT) to DMAB.[115, 116] It was shown that a lower threshold was required for graphene/Au SERS substrate than pure Au nanoparticles, given the same experimental conditions. Similarly, Wu et al. investigated the formation of DMAB on Ag nanoparticles/graphene oxide nanocomposites.[117]

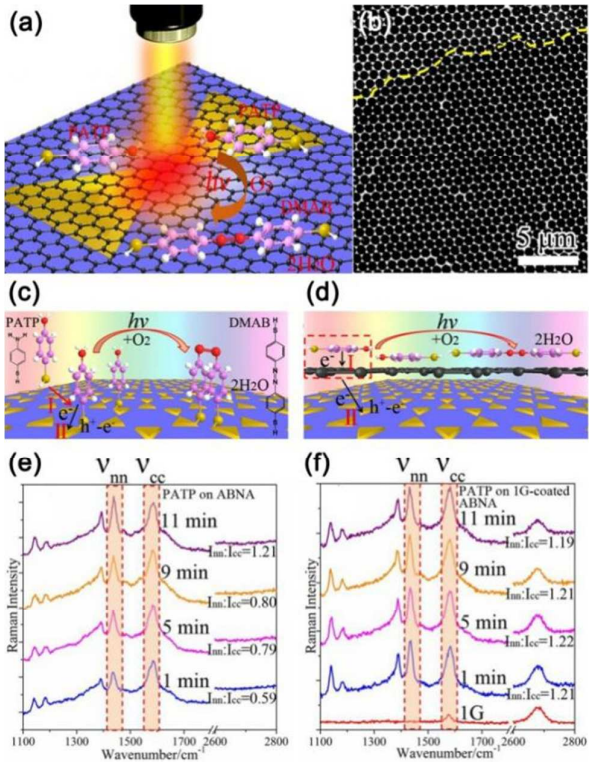

Fig. 13 (a) Schematic illustration of plasmon-driven catalytic reaction of transforming PATP to DMAB on SLG-coated ABNA; (b) SEM image of large-area graphene-covered ABNA (below the yellow dashed line); Schematic view of the formation process of DMAB on (c) plasmonic metal and (d) graphene mediated SERS substrate; Time-dependent Raman spectra of 4ATP on (e) ABNA and (f) SLG-covered ABNA. Adapted from submitted manuscript.[114]

One can see that graphene, employed as an efficient mediator to investigate the plasmon-driven reaction, is still in its infancy, but it is believed that the new role of graphene in plasmon-driven catalytic reactions will attract more and more attentions, and more useful catalytic reactions might be realized with this technique.

Conclusions and outlook

This review focused on the recent applications of graphene in SERS and plasmon-driven chemical reactions, from many other unique properties of this 2D material. Undoubtedly, graphene has played an important role in SERS and is expected to make a breakthrough in future studies to meet the practical applications, though this could not be accomplished in an action. For example, reproducible Raman signals can be collected from graphene surface, but enhancement factor is rather low for GERS comparing with conventional SERS technique. From application point of view, a careful balance the relationship among sensitivity, selectivity and reproducibility is required to be preferentially considered. On the basis of the unique properties of graphene, the ingenious integration of graphene with well-defined metal nanostructures would be one of the reliable choices. Furthermore, it should be noted that the chemically inert graphene could be modified by laser illumination in different surroundings, even in moisture air, and these changes would further affect the SERS signals from them. Also, the high electron mobility of graphene is often neglected in SERS. It has been demonstrated that graphene can be an efficient mediator to accelerate the plasmon-driven catalytic reactions. In-depth investigations of graphene-related Raman enhancement will be beneficial for providing deep insight into not only promising SERS substrate but also chemical enhancement mechanism. And laser-induced reactions on graphene and graphene mediated catalytic reactions remind researchers of these adverse influences to G-SERS and GERS. We believe that the function of graphene in both SERS and plasmon-driven catalytic reactions will draw more and more attention in the near future. In addition, driven by the development of graphene in SERS field, other 2D materials are being exploited to boost the progress of SERS technique.

Acknowledgements

We thank the financial supporting from NSFC (No. 21471039, 91436102,21203045, 11374353), Fundamental Research Funds for the Central Universities (Grant No. HIT. NSRIF. 2010065 and2011017, PIRS of HIT A201502 and HIT. BRETIII. 201223), China Postdoctoral Science Foundation (2014M560253), Postdoctoral Scientific Research Fund of Heilongjiang Province (LBH-Q14062, LBH-Z14076), Open Project Program of Key Laboratory for Photonic and Electric Bandgap Materials, Ministry of Education, Harbin Normal University, China (PEBM 201306), and Open Foundation of State Key Laboratory of Electronic Thin Films and Integrated Devices (KFJJ201401) and the Program of Liaoning Key Laboratory of Semiconductor Light Emitting and Photocatalytic Materials.

References

1. K. Novoselov, A. Geim, S. Morozov, D. Jiang, Y. Zhang, S. Dubonos, I. Grigorieva and A. Firsov, *Science*, 2004, **306**, 666-669.
2. P. Yin, S. Shah, M. Chhowalla and K. Lee, *Chem. Rev.*, 2015, **115**, 2483-2531.
3. A. Geim and K. Novoselov, *Nat. Mater.*, 2007, **6**, 183-191.
4. Z. Wang, H. Zeng and L. Sun, *J. Mater. Chem. C*, 2015, **3**, 1157-1165.
5. Y. Hernandez, V. Nicolosi, M. Lotya, F. Blighe, Z. Sun, S. De, I. McGovern, B. Holland, M. Byrne, Y. Gun'ko, J. Boland, P. Niraj, G. Duesberg, S. Krishnamurthy, R. Goodhue, J. Hutchison, V. Scardaci, A. Ferrari and J. Coleman, *Nat. Nanotechnol.*, 2008, **3**, 563-568.

6. P. Blake, P. Brimicombe, R. Nair, T. Booth, D. Jiang, F. Schedin, L. Ponomarenko, S. Morozov, H. Gleeson, E. Hill, A. Geim and K. Novoselov, *Nano Lett.*, 2008, **8**, 1704-1708.
7. X. Li, W. Cai, J. An, S. Kim, J. Nah, D. Yang, R. Piner, A. Velamakanni, I. Jung, E. Tutuc, S. K. Banerjee, L. Colombo and R. S. Ruoff, *Science*, 2009, **324**, 1312-1314.
8. J. Hackley, D. Ali, J. DiPasquale, J. D. Demaree and C. J. K. Richardson, *Appl. Phys. Lett.*, 2009, **95**, 133114.
9. K. Novoselov, V. Fal'ko, L. Colombo, P. Gellert, M. Schwab and K. Kim, *Nature*, 2012, **490**, 192-200.
10. L. Guerrini and D. Graham, *Chem. Soc. Rev.*, 2012, **41**, 7085-7107.
11. A. Campion and P. Kambhampati, *Chem. Soc. Rev.*, 1998, **27**, 241-250.
12. H. Xu, J. Aizpurua, M. Kall and P. Apell, *Phys. Rev. E*, 2000, **62**, 4318-4324.
13. L. Kang, X. Han, J. Chu, J. Xiong, X. He, H. L. Wang and P. Xu, *ChemCatChem*, 2015, **7**, 1004-1010.
14. X. Ji and W. Yang, *Chem. Sci.*, 2014, **5**, 311-323.
15. H. Fu, X. Lang, C. Hou, Z. Wen, Y. Zhu, M. Zhao, J. Li, W. Zheng, Y. Liu and Q. Jiang, *J. Mater. Chem. C*, 2014, **2**, 7216-7222.
16. J. Li, Y. Huang, Y. Ding, Z. Yang, S. B. Li, X. Zhou, F. Fan, W. Zhang, Z. Zhou, Y. Wu de, B. Ren, Z. Wang and Z. Tian, *Nature*, 2010, **464**, 392-3955.
17. X. Ling, L. Xie, Y. Fang, H. Xu, H. Zhang, J. Kong, M. S. Dresselhaus, J. Zhang and Z. Liu, *Nano Lett.*, 2010, **10**, 553-561.
18. X. Ling and J. Zhang, *J. Phys. Chem. C*, 2011, **115**, 2835-2840.
19. W. Xu, N. Mao and J. Zhang, *Small*, 2013, **9**, 1206-1224.
20. E. Koo and S. Ju, *Carbon*, 2015, **86**, 318-324.
21. P. Klar, E. Lidorikis, A. Eckmann, I. Verzhbitskiy, A. Ferrari and C. Casiraghi, *Phys. Rev. B*, 2013, **87**, 205435.
22. A. Ferrari, J. Meyer, V. Scardaci, C. Casiraghi, M. Lazzeri, F. Mauri, S. Piscanec, D. Jiang, K. Novoselov, S. Roth and A. Geim, *Phys. Rev. Lett.*, 2006, **97**, 187401.
23. J. Wu, H. Xu and J. Zhang, *Acta Chimica Sinica*, 2014, **72**, 301-318.
24. J. Maultzsch, S. Reich and C. Thomsen, *Phys. Rev. B*, 2004, **70**, 155403.
25. A. Ferrari and D. Basko, *Nat. Nanotechnol.*, 2013, **8**, 235-246.
26. L. Malard, M. Pimenta, G. Dresselhaus and M. Dresselhaus, *Phys. Rep.*, 2009, **473**, 51-87.
27. M. Iqbal, M. Khan, M. Iqbal and J. Eom, *J. Mater. Chem. C*, 2014, **2**, 5404-5410.
28. C. Casiraghi, A. Hartschuh, H. Qian, S. Piscanec, C. Georgi, A. Fasoli, K. Novoselov, D. Basko and A. Ferrari, *Nano Lett.*, 2009, **9**, 1433-1441.
29. M. Bruna, A. Ott, M. Ijaes, D. Yoon, U. Sassi and A. Ferrari, *Acs Nano*, 2014, **8**, 7432-7441.
30. Q. Li, X. Zhang, W. Han, Y. Lu, W. Shi, J. Wu and P. Tan, *Carbon*, 2015, **85**, 221-224.
31. P. Tan, W. Han, W. Zhao, Z. Wu, K. Chang, H. Wang, Y. Wang, N. Bonini, N. Marzari and N. Pugno, *Nat. Mater.*, 2012, **11**, 294-300.
32. P. Stiles, J. Dieringer, N. Shah and R. Van Duyne, *Annu. Rev. Anal. Chem.*, 2008, **1**, 601-626.
33. M. Liu, H. Zhao, X. Quan, S. Chen and X. Fan, *Chem. Commun.*, 2010, **46**, 7909-7911.
34. X. Guo, Z. Ni, C. Liao, H. Nan, Y. Zhang, W. Zhao and W. Wang, *Appl. Phys. Lett.*, 2013, **103**, 201909.
35. Z. Liu, Y. Xu, X. Zhang, X. Zhang, Y. Chen and J. Tian, *J. Phys. Chem. B*, 2009, **113**, 9681-9686.
36. C. Zhang, Y. Yuan, S. Zhang, Y. Wang and Z. Liu, *Angew. Chem. Int. Edit.*, 2011, **50**, 6851-6854.
37. R. Swathi and K. Sebastian, *J. Chem. Phys.*, 2009, **130**, 086101.
38. L. Xie, X. Ling, Y. Fang, J. Zhang and Z. Liu, *J. Am. Chem. Soc.*, 2009, **131**, 9890-9891.
39. M. Fleischmann, P. Hendra and A. McQuillan, *Chem. Phys. Lett.*, 1974, **26**, 163-166.
40. A. Hakonen, M. Svedendahl, R. Ogier, Z. Yang, K. Lodewijks, R. Verre, T. Shegai, P. Andersson and M. Käll, *Nanoscale*, 2015, **7**, 9405-9410.
41. J. Wang, F. Zhou, G. Duan, Y. Li, G. Liu, F. Su and W. Cai, *RSC Adv.*, 2014, **4**, 8758-8763.
42. M. Cecchini, V. Turek, J. Paget, A. Kornyshev and J. Edel, *Nat. Mater.*, 2013, **12**, 165-171.
43. L. Kang, P. Xu, D. Chen, B. Zhang, Y. Du, X. Han, Q. Li and H. Wang, *J. Phys. Chem. C*, 2013, **117**, 10007-10012.
44. P. Xu, X. Han, B. Zhang, Y. Du and H. Wang, *Chem. Soc. Rev.*, 2014, **43**, 1349-1360.
45. B. Zhang, P. Xu, X. Xie, H. Wei, Z. Li, N. H. Mack, X. Han, H. Xu and H. Wang, *J. Mater. Chem.*, 2011, **21**, 2495-2501.
46. S. Schluecker, *Angew. Chem. Int. Edit.*, 2014, **53**, 4756-4795.
47. S. Kleinman, R. Frontiera, A. Henry, J. Dieringer and R. Van Duyne, *Phys. Chem. Chem. Phys.*, 2013, **15**, 21-36.
48. F. Schedin, E. Lidorikis, A. Lombardo, V. Kravets, A. Geim, A. Grigorenko, K. Novoselov and A. Ferrari, *Acs Nano*, 2010, **4**, 5617-5626.
49. Y. Lee, E. Wang, Y. Liu and H. Chen, *Chem. Mater.*, 2015.
50. J. Lee, K. S. Novoselov and H. S. Shin, *Acs Nano*, 2011, **5**, 608-612.
51. P. Wang, W. Zhang, O. Liang, M. Pantoja, J. Katzer, T. Schroeder and Y. Xie, *Acs Nano*, 2012, **6**, 6244-6249.
52. P. Wang, O. Liang, W. Zhang, T. Schroeder and Y. H. Xie, *Adv. Mater.*, 2013, **25**, 4918-4924.
53. M. Losurdo, I. Bergmair, B. Dastmalchi, T.-H. Kim, M. M. Giangregroio, W. Jiao, G. V. Bianco, A. S. Brown, K. Hingerl and G. Bruno, *Adv. Funct. Mater.*, 2014, **24**, 1864-1878.
54. W. Xu, X. Ling, J. Xiao, M. Dresselhaus, J. Kong, H. Xu, Z. Liu and J. Zhang, *Proc. Natl. Acad. Sci. U. S. A.*, 2012, **109**, 9281-9286.
55. W. Xu, J. Xiao, Y. Chen, Y. Chen, X. Ling and J. Zhang, *Adv. Mater.*, 2013, **25**, 928-933.
56. X. Zhu, L. Shi, M. S. Schmidt, A. Boisen, O. Hansen, J. Zi, S. Xiao and N. A. Mortensen, *Nano Lett.*, 2013, **13**, 4690-4696.
57. A. Liu, T. Xu, J. Tang, H. Wu, T. Zhao and W. Tang, *Electrochimica Acta*, 2014, **119**, 43-48.
58. L. Zhang, C. Jiang and Z. Zhang, *Nanoscale*, 2013, **5**, 3773-3779.
59. T. Gong, Y. Zhu, J. Zhang, W. Ren, J. Quan and N. Wang, *Carbon*, 2015, **87**, 385-394.

60. X. Li, W. C. H. Choy, X. Ren, D. Zhang and H. Lu, *Adv. Funct. Mater.*, 2014, **24**, 3114-3122.
61. Y. Zhao, W. Zeng, Z. Tao, P. Xiong, Y. Qu and Y. Zhu, *Chem. Commun.*, 2015, **51**, 866-869.
62. S. Xu, B. Man, S. Jiang, J. Wang, J. Wei, S. Xu, H. Liu, S. Gao, H. Liu and Z. Li, *ACS Appl. Mater. Inter.*, 2015, **7**, 10977-10987.
63. Y. Liu, Y. Hu and J. Zhang, *J. Phys. Chem. C*, 2014, **118**, 8993-8998.
64. R. Lu, A. Konzelmann, F. Xu, Y. Gong, J. Liu, Q. Liu, M. Xin, R. Hui and J. Z. Wu, *Carbon*, 2015, **86**, 78-85.
65. K. Turcheniuk, R. Boukherroub and S. Szunerits, *J. Mater. Chem. B*, 2015, **3**, 4301-4324.
66. H. Qiu, S. Xu, P. Chen, S. Gao, Z. Li, C. Zhang, S. Jiang, M. Liu, H. Li and D. Feng, *Appl. Surf. Sci.*, 2015, **332**, 614-619.
67. M. Jiang, Z. Qian, X. Zhou, X. Xin, J. Wu, C. Chen, G. Zhang, G. Xu and Y. Cheng, *Phys. Chem. Chem. Phys.*, 2015, DOI: 10.1039/C4CP04888A.
68. Y. Zhao, W. Zeng, Z. Tao, P. Xiong, Y. Qu and Y. Zhu, *Chem. Commun.*, 2015, **51**, 866-869.
69. X. Ling, L. G. Moura, M. A. Pimenta and J. Zhang, *J. Phys. Chem. C*, 2012, **116**, 25112-25118.
70. X. Ling, J. Wu, L. Xie and J. Zhang, *J. Phys. Chem. C*, 2013, **117**, 2369-2376.
71. S. Huh, J. Park, Y. S. Kim, K. S. Kim, B. H. Hong and J.-M. Nam, *Acs Nano*, 2011, **5**, 9799-9806.
72. X. Yu, H. Cai, W. Zhang, X. Li, N. Pan, Y. Luo, X. Wang and J. Hou, *Acs Nano*, 2011, **5**, 952-958.
73. J. Liu, H. Cai, X. Yu, K. Zhang, X. Li, J. Li, N. Pan, Q. Shi, Y. Luo and X. Wang, *J. Phys. Chem. C*, 2012, **116**, 15741-15746.
74. Y. Wang, Z. Ni, A. Li, Z. Zafar, Y. Zhang, Z. Ni, S. Qu, T. Qiu, T. Yu and Z. X. Shen, *Appl. Phys. Lett.*, 2011, **99**, 233103
75. S. Sun and P. Wu, *Phys. Chem. Chem. Phys.*, 2011, **13**, 21116-21120.
76. S. Huang, X. Ling, L. Liang, Y. Song, W. Fang, J. Zhang, J. Kong, V. Meunier and M. S. Dresselhaus, *Nano Lett.*, 2015, **15**, 2892-2901.
77. H. Xu, L. Xie, H. Zhang and J. Zhang, *Acs Nano*, 2011, **5**, 5338-5344.
78. X. Ling and J. Zhang, *Small*, 2010, **6**, 2020-2025.
79. H. Xu, Y. Chen, W. Xu, H. Zhang, J. Kong, M. Dresselhaus and J. Zhang, *Small*, 2011, **7**, 2945-2952.
80. X. Ling, J. Wu, W. Xu and J. Zhang, *Small*, 2012, **8**, 1365-1372.
81. R. Lv, Q. Li, A. Botello-Méndez, T. Hayashi, B. Wang, A. Berkdemir, Q. Hao, A. Elías, R. Cruz-Silva and H. Gutiérrez, *Sci. Rep.*, 2012, **2**, 586.
82. V. Sangwan, D. Jariwala, I. Kim, K. Chen, T. Marks, L. Lauhon and M. Hersam, *Nat. Nanotechnol.*, 2015, **10**, 403-406.
83. R. Koitz, J. Nørskov and F. Studt, *Phys. Chem. Chem. Phys.*, 2015, **17**, 12722-12727.
84. X. Ling, W. Fang, Y. Lee, P. Araujo, X. Zhang, J. Rodriguez-Nieva, Y. Lin, J. Zhang, J. Kong and M. Dresselhaus, *Nano Lett.*, 2014, **14**, 3033-3040.
85. W. Ji, Y. Kitahama, X. Xue, B. Zhao and Y. Ozaki, *J. Phys. Chem. C*, 2012, **116**, 2515-2520.
86. Y. Guo, L. Kang, S. Chen and X. Li, *Phys. Chem. Chem. Phys.*, 2015, DOI: 10.1039/c5cp00206k.
87. L. Xia, M. Chen, X. Zhao, Z. Zhang, J. Xia, H. Xu and M. Sun, *J. Raman Spectrosc.*, 2014, **45**, 533-540.
88. M. Bruna and S. Borini, *Appl. Phys. Lett.*, 2009, **94**, 031901.
89. E. Thrall, A. Crowther, Z. Yu and L. Brus, *Nano Lett.*, 2012, **12**, 1571-1577.
90. J. R. Lombardi, R. L. Birke, T. H. Lu and J. Xu, *J. Chem. Phys.*, 1986, **84**, 4174-4180.
91. B. N. J. Persson, K. Zhao and Z. Y. Zhang, *Phys. Rev. Lett.*, 2006, **96**, 207401.
92. E. Barros and M. Dresselhaus, *Phys. Rev. B*, 2014, **90**, 035443.
93. S. Schlucker, *Angew. Chem. Int. Edit.*, 2014, **53**, 4756-4795.
94. Y. Fang, Y. Li, H. Xu and M. Sun, *Langmuir*, 2010, **26**, 7737-7746.
95. Y. Huang, H. Zhu, G. Liu, D. Wu, B. Ren and Z. Tian, *J. Am. Chem. Soc.*, 2010, **132**, 9244-9246.
96. L. Kang, P. Xu, B. Zhang, H. Tsai, X. Han and H. Wang, *Chem. Commun.*, 2013, **49**, 3389-3391.
97. Y. Huang, M. Zhang, L. Zhao, J. Feng, D. Wu, B. Ren and Z. Tian, *Angew. Chem. Int. Edit.*, 2014, **53**, 2353-2357.
98. B. Dong, Y. Fang, X. Chen, H. Xu and M. Sun, *Langmuir*, 2011, **27**, 10677-10682.
99. L. Cui, P. Wang, X. Chen, Y. Fang, Z. Zhang and M. Sun, *Sci. Rep.*, 2014, **4**, 7221.
100. M. Sun, Z. Zhang, L. Chen, Q. Li, S. Sheng, H. Xu and P. Song, *Adv. Mater. Interfaces*, 2014, **1**, 1300125.
101. X. Zhang, P. Wang, Z. Zhang, Y. Fang and M. Sun, *Sci. Rep.*, 2014, **4**, 5407.
102. W. Huang, Q. Jing, Y. Du, B. Zhang, X. Meng, M. Sun, K. Schanze, H. Gao and P. Xu, *J. Mater. Chem. C*, 2015, **3**, 5285-5291.
103. D. Elias, R. Nair, T. Mohiuddin, S. Morozov, P. Blake, M. Halsall, A. Ferrari, D. Boukhvalov, M. Katsnelson and A. Geim, *Science*, 2009, **323**, 610-613.
104. W. Lee, J. Suk, H. Chou, J. Lee, Y. Hao, Y. Wu, R. Piner, D. Akinwande, K. Kim and R. Ruoff, *Nano Lett.*, 2012, **12**, 2374-2378.
105. L. Zhou, M. Yang, D. Wu, L. Liao, K. Yan, Q. Xie, Z. Liu and H. Peng, *Small*, 2013, **9**, 1388-1396.
106. B. Li, L. Zhou, D. Wu, H. Peng, K. Yan, Y. Zhou and Z. Liu, *Acs Nano*, 2011, **5**, 5957-5961.
107. M. Z. Hossain, M. B. A. Razak, H. Noritake, Y. Shiozawa, S. Yoshimoto, K. Mukai, T. Koitaya, J. Yoshinobu and S. Hosaka, *J. Phys. Chem. C*, 2014, **118**, 22096-22101.
108. L. Liao, Z. Song, Y. Zhou, H. Wang, Q. Xie, H. Peng and Z. Liu, *Small*, 2013, **9**, 1348-1352.
109. H. Liu, S. Ryu, Z. Chen, M. L. Steigerwald, C. Nuckolls and L. E. Brus, *J. Am. Chem. Soc.*, 2009, **131**, 17099-17101.
110. N. Mitoma, R. Nouchi and K. Tanigaki, *J. Phys. Chem. C*, 2013, **117**, 1453-1456.
111. P. Xu, L. Kang, N. H. Mack, K. S. Schanze, X. Han and H.-L. Wang, *Sci. Rep.*, 2013, **3**, 2997.
112. D. A. Sokolov, K. R. Shepperd and T. M. Orlando, *J. Phys. Chem. Lett.*, 2010, **1**, 2633-2636.
113. Y. Zhang, L. Guo, H. Xia, Q. Chen, J. Feng and H. Sun, *Adv. Opt. Mater.*, 2014, **2**, 10-28.
114. Z. Dai, X. Xiao, W. Wu, Y. Zhang, L. Liao, S. Guo, J. Ying, C. Shan, M. Sun and C. Jiang, *Light-Sci. Appl.* 2015, **4**, e342.

115.X. Liang, T. You, D. Liu, X. Lang, E. Tan, J. Shi, P. Yin and L. Guo, *Phys. Chem. Chem. Phys.*, 2015, **17**, 10176-10181.
116.J. Li, C. Liu and Y. Liu, *J. Mater. Chem.*, 2012, **22**, 8426-8430.
117.H.-Y. Wu, Y.-H. Lai, M.-S. Hsieh, S.-D. Lin, Y.-C. Li and T.-W. Lin, *Adv. Mater. Interfaces*, 2014, **1**, 1400119.

Author Biography

Leilei Kang was born in Shanxi, China. He received his MS degree in Inorganic Chemistry from Harbin Institute of Technology in 2010 and is now a PhD candidate with Prof. Ping Xu. His current research is concentrated on the fabrication of SERS substrates and in situ SERS study of plasmon-driven catalytic reactions.

Jiayu Chu was born in Heilongjiang, China. She received her BS from Qiqihar University in 2013. She is now a PhD candidate with Prof. Ping Xu at Harbin Institute of Technology. Her current research is focused on SERS and surface plasmon-driven catalytic reactions on metal-semiconductor nanocomposites.

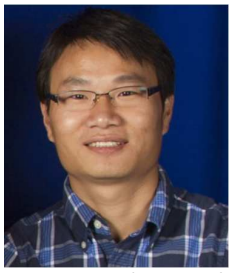

Ping Xu was born in Zhejiang, China. He received a BS degree in Applied Chemistry (2003) and a PhD degree in Chemical Engineering and Technology (2010) from the Harbin Institute of Technology (HIT). He spent one year (2008-2009) as a visiting student and one and a half years (2012-2013) as a Director's Postdoctoral Fellow at Los Alamos National Laboratory (LANL). He started as an Assistant Professor at HIT in 2010, and was promoted to Associate Professor in 2013 and to Full Professor in 2014. His current research interests include design and synthesis of nanostructured materials and hybrid materials for applications in surface enhanced Raman spectroscopy; surface plasmon assisted catalysis, and advanced energy devices.

Mengtao Sun is an Associate Professor at the Institute of Physics, Chinese Academy of Sciences (CAS). He obtained his Ph.D. in 2003 from State Key Laboratory of Molecular Reaction Dynamics, Dalian Institute of Chemical Physics, CAS, working on optical-optical double resonance multiphoton ionization spectroscopy. From 2003 to 2006, he worked as a postdoc at the Department of Chemical Physics, Lund University, working on the photoinduced charge transfer in organic solar cells. Since 2006, he works at the Institute of Physics, CAS. His current research interests focus on HV-TERS, SERS and G-SERS, and plasmon driven chemical reactions.

Graphical Abstract

In this review, we mainly focus on the state-of-the-art applications of graphene in the fields of Surface-enhanced Raman scattering (SERS) and plasmon-induced catalytic reactions. The advances of informative Raman spectra of graphene are firstly reviewed. Then, the graphene related SERS substrates, including graphene-enhanced Raman scattering (GERS) and graphene-mediated SERS (G-SERS), are summarized. We finally highlight the catalytic reactions occurring on graphene itself and molecules adsorbed onto graphene upon laser irradiation.